ECE 445

SENIOR DESIGN LABORATORY

FINAL REPORT

EEG Drowsiness Detection Device

Team #28

SENTURRAN ELANGOVAN
(se10@illinois.edu)
NIKHIL TALWALKAR
(nikhilt4@illinois.edu)

TA: Zhuoer Zhang

December 10, 2025

Abstract

Drowsiness-related accidents pose a significant safety risk in transportation, shift work, and other fatigue-prone environments. This design suggests a wearable EEG-based drowsiness detector as a tool to provide real-time monitoring and rapid alerting preventing microsleeps. The device integrates reusable forehead electrodes, an ADS1299 biopotential ADC, and STM32F412RGT6 microcontroller to acquire and process brainwave signals continuously. Our firmware implements on-board digital signal processing, including windowing, power-ratio analysis of theta and alpha bands, and a dynamic thresholding algorithm tailored to each user. When drowsiness is detected, a low-power piezoelectric buzzer provides an immediate warning. The system is powered by a compact Li-Po battery with an integrated BMS and dual-stage voltage regulation to ensure safe and stable operation for extended wear. Despite practical constraints in cost, time, and component availability, the final prototype demonstrates reliable EEG acquisition, effective drowsiness detection across multiple users, and prompt alert activation, validating the feasibility of an accessible, portable neurotechnology-based safety tool.

Contents

1 Introduction

1.1 Problem

Drowsiness is an extensive safety risk in shift-work, transportation occupations, or night-time operations (eg, nurses, night-shift operators, and drivers). An estimate from the NHTSA says in 2017 reported 91,000 police-reported crashes, 50,000 injuries, and approximately 800 deaths involving drowsy drivers[1]. They also acknowledged these statistics are an underestimate of the impact of drowsy driving [1]. More recently, NHTSA reports on their website a total of 633 drowsy-driving-related deaths[1]. Surveys cited by the National Safety Commission show about 1 in 25 adults report of having falling asleep while driving in the past month [2], suggesting a much larger problem than factual surveys and reports can estimate.

In these situations where people may be subject to moments of fatigue or loss of focus, the consequences can result in catastrophic accidents. What if there is a device that can make sure we are alert at late hours or extreme exhaustion?

1.2 Solution

An electroencephalogram (EEG)-based drowsiness detector could be an assistive solution to these problems by continuously monitoring brain activity and alerting users at the onset of sleepiness. EEGs are a non-invasive medical device that measures brainwaves rather than relying on visual proxies such as blink rates, head positions or body posture. Our design integrates real-time EEG acquisition into a compact, wearable device capable of functioning with minimal obstruction to daily routines.

This technology is designed to constantly monitor the brain waves of the user and alert them back into consciousness when a change in pattern is detected. This bridges the gap between neuroscience and practical safety applications, offering a potentially life-saving tool in environments where attention is necessary.

1.3 High Level Requirements

- **EEG acquisition:** The device must capture EEG signals with sufficient accuracy to reliably register events associated with drowsiness and microsleep. This can be tested through eye blinks which provide a detectable and significant voltage spike above baseline noise.
- **Real-time drowsiness detection:** The system must detect micro-sleeps or drowsiness with at least 90% accuracy and a low false positive rate when tested during user trials.
- **Prompt alerting:** The alert mechanism (buzzer) must activate within a timely manner <= 2 seconds) from the onset of detected drowsiness, measured by comparing EEG event timestamp with the output signal.

- **Wearability and safety:** The device must remain safe and comfortable for at least 8 continuous hours. We will verify this through randomly selected volunteers and quantify comfort through a number scale (1-5). For the product to pass, the average comfort level should be a 4/5.

1.4 Visual Representation

Our design for our device can be found in Figure 9 of the appendix. It shows a fabric cap with 3 electrodes mounted by the forehead. The box of the our device sits at the top, with a buzzer on the side by the ear.

2 Design

2.1 Block Diagram

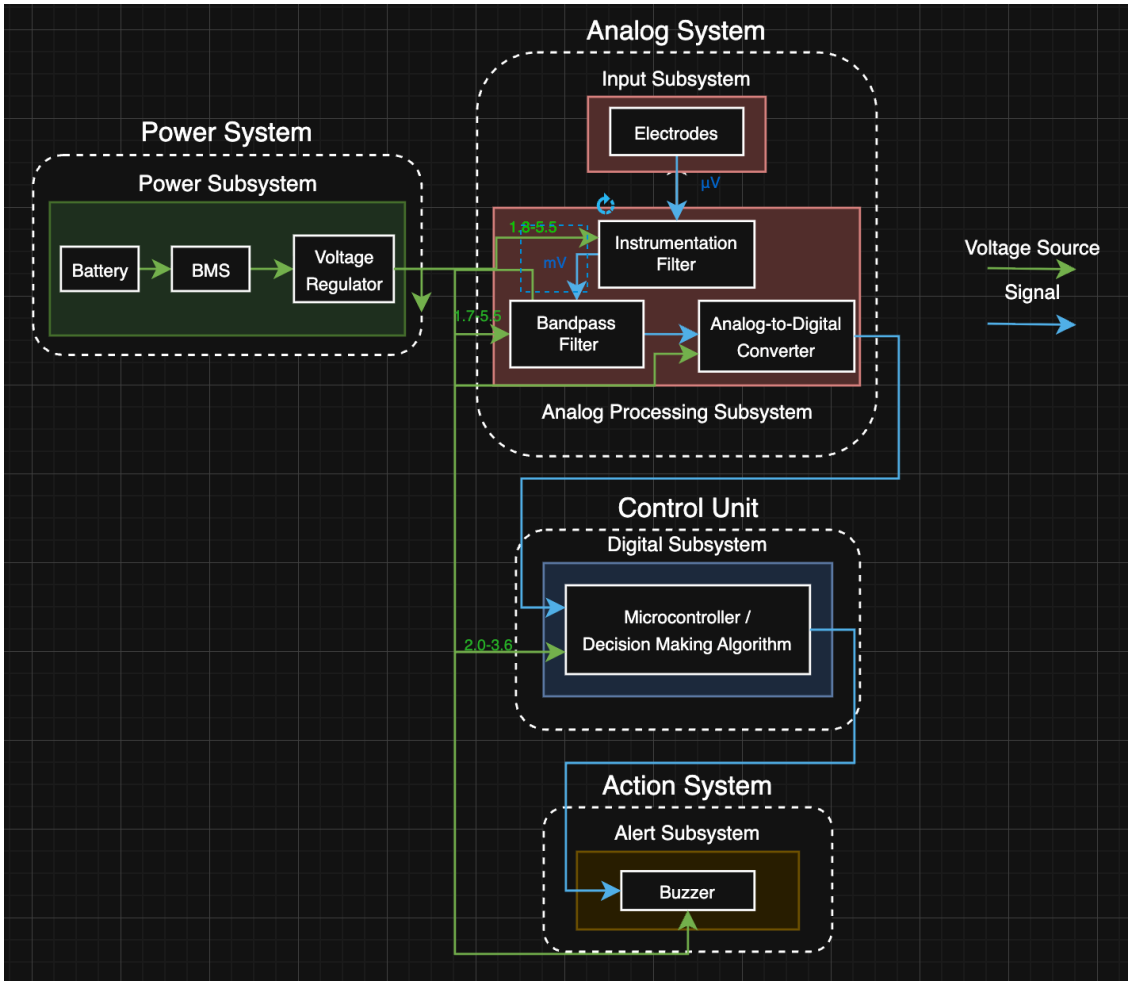

Figure 1: Block diagram of the system highlighting the subsystems and their interconnections

The block diagram highlights 4 main subsystems. The power subsystem, the signal acquisition subsystem(also labeled as the analog system), the control subsystem and the action subsystem. The power subsystem provides power to the system as whole, with a battery, battery management system(BMS), and a voltage regulator. The signal acquisition subsystem is comprised of electrodes and an analog-to-digital converter(ADS1299). The electrodes picks up the signal from the person and the ADC chip (ADS1299) processes the signal, making it suitable for the next step, the digital processing. The digital processing is mainly done by the STM32F412RGT6. It uses digital signal processing and hysteresis to carry out the decision-making process, finalizing whether the buzzer needs to be sounded or not. Eventually, the buzzer will be activated to make noise by the STM32F412RGT6 when it detects microsleeps or drowsiness.

2.2 Power System

The power system consists of a Lithium-Polymer (Li-Po) battery integrated with a Battery Management System (BMS), a boost converter, and a buck converter. Li-Po batteries were chosen for their high energy density, light weight, and compact form factor, allowing the battery (34.5 × 51 × 6.3 mm, W×L×H) to fit seamlessly into the headband design. The nominal voltage of 3.7 V (operating range: 3.2–4.2 V) is compatible with most components, and the initial minimum capacity of $3600mAh$ provides a battery life exceeding 8 hours. However, due to cost and availability, the battery capacity finally chosen was $3000mAh$ bringing expected battery life to decrease a little. The battery is rechargeable and designed for easy replacement. While Li-Po batteries offer many advantages, they are sensitive to high temperatures and can be damaged by overcharging or over-discharging. This is where the BMS comes into play.

The BMS ensures safe operation by keeping the battery within its rated operating region, limiting both charging and discharging currents. The cascaded LM317 regulator restricts the current flowing into and out of the battery, while the BD140 transistor functions as a switch that disconnects the supply once the battery reaches its rated peak voltage of 4.2 V. At this point, the excess power is diverted to the diodes, lighting up an LED to signal that the battery is fully charged. A USB-A module is included to provide users with a convenient charging interface. A 1 A fuse and a capacitor are added near the input to suppress large current spikes and protect the circuit and power supply.

Additionally, a voltage regulation stage is implemented to provide the necessary voltages for the STM32F412RGT6 and ADS1299. The ADS1299 requires a 5 V analog rail and a 3.3 V digital rail, while the STM32F412RGT6 and the buzzer are both powered at 3.3 V. To achieve this, a boost converter steps up the nominal 3.7 V battery voltage to a stable 5 V, followed by a buck converter that steps it down to 3.3 V. This configuration ensures both required voltages are supplied with improved efficiency and stability.

2.3 Analog System

The signal acquisition subsystem is composed of reusable EEG electrodes, snap electrode cables, and a bio-potential-specific analog-to-digital converter (ADC), the ADS1299. The electrodes chosen are flat snap EEG electrodes (TDE-202), which are inexpensive, reusable, and widely adopted for non-medical EEG applications. They provide a reasonable trade-off between cost and signal accuracy. The flat snap lead wires are lightweight, well-shielded, and can be integrated neatly into the headband design. The acquired EEG signal is filtered using a first layer of RC filters that filter any frequency above $24Hz$ chosen using the given equation 2.1 before being supplied to the analog-to-digital converter, ADS1299.

$$f_{cutoff} = \frac{1}{2\pi R_{eff} C_{eff}}[Hz] \tag{1}$$

The ADS1299 is designed to accurately measure small bio potential signals such as EEG by minimizing external interference and common-mode noise. It features high common-mode rejection through its differential input amplifiers, which effectively cancel out noise

that appears equally on both inputs, such as power line interference from the 60 Hz mains supply. Additionally, the ADS1299 includes an internal bias amplifier that computes the average of all electrode voltages, inverts this signal, and drives it back into the body through the bias electrode. This feedback loop actively stabilizes the body's potential and reduces common-mode noise before it even reaches the ADC inputs. Together, these mechanisms ensure that only the true differential EEG signals—primarily in the 0.5–$13\ Hz$ range—are preserved, while unwanted high-frequency or common-mode noise is strongly suppressed, resulting in a cleaner and more accurate neural recording.

2.4 Control Unit

The controller system is a microcontroller that ingests digital EEG samples from the ADS1299, executes our real-time processing and decision algorithm, and alerts the Alarm system (buzzer) based on the drowsiness detection. Upstream, it will interface to the ADS1299 via SPI (Serial Peripheral Interface) with data-ready interrupts and control sets. Downstream, it outputs a GPIO (General Purpose Input/Output) control signal to the buzzer. Internally, it will perform digital signal processing such as band-pass filtering, windowing and heuristic decision making.

We will be using the STM32F412RGT6 chip for our microcontroller. We chose this chip as it's a well-supported Cortex M4 with tons of open-source examples, STM32CubeIDE libraries, and clear documentation. Its fast and relatively low risk to develop in our short time frame. It has no WiFi/ Bluetooth (which is good for EEG safety and privacy) and has plenty of flash and RAM memory (1MB/256KB respectively). These all make it a perfect chip for real-time DSP and keep our product isolated from outside sources for better privacy and safety of users.

The schematic below shows our design. The STM chip connects to the ADS1299 via a standard link and 'data-ready' line to make sure data is only read when new samples are available. It also provides clock signals for the ADS through SCK. For our alarm system, the chip provides a simple GPIO output to the active buzzer to play a tune when drowsiness is detected. Our breadboard demo demonstrated the high volume and effectiveness of the buzzer sound through a nucleo board. Through STM32Cube software, we can produce any type of single-tone tunes and beats which will be tested later in the future. Power is provided from the battery system with a 3.3V line. Decoupling capacitors will be placed all around the microchip.

2.5 Action System

The alarm system uses a small and low-power active piezoelectric buzzer to alert the user when the device detects drowsiness. Since the buzzer can be placed close to the ears, it does not require large voltages to produce loud noises; instead, a smaller voltage is

enough for a loud and alerting tune. This design reduces user discomfort and helps conserve battery power.

The MCU controls the buzzer through a GPIO pin, sending a signal to the buzzer as soon as the algorithm detects any drowsiness or micro-sleep. The piezoelectric buzzer is rated to draw 15 mA of current at 3.3 V. We aim to operate the buzzer at lower voltages, hence lower power consumption and longer battery life.

2.6 Firmware and Digital Signal Processing

The firmware running on the STM32 microchip implements digital signal processing, drowsiness detection logic and generating alerts. The software turns EEG samples from the ADS1299 to monitor the user's drowsiness state in real time. All processing is performed on-board to minimize response time and maximize user privacy and safety.

2.6.1 Sampling, buffering and windowing

The STM32 microchip communicated over SPI with the ADS1299 to receive signals. The data ready (DRDY) pin generates an external interrupt which produces a new 24-bit frame of data infinitely.

Samples are stored in a buffer of length 256 corresponding to around 1.024 seconds. These form 256 size windows processed by the firmware. This is configured by setting ADS1299 registers to a 250Hz sampling rate. However, to the make the processing even faster, as individual windows are processed, the buffer updates and processes a new window every 128 samples. This result in a half second update rate and much faster decision making.

2.6.2 Power ratios

Our drowsiness metric is based on the power ratings of specific frequency bands theta (6Hz) and alpha (10Hz). These two waves' can increase in amplitude during eye closure and early sleep which we are tracking.

The first step is to remove any DC offset to standardize and improve our ADC range. The equation below is a calculation of the mean across the whole sample, and subtracting each sample from that mean to center it at 0:

$$x_{\text{center}}[n] = x[n] - \frac{1}{N}\sum_{k=0}^{N-1} x[k] \tag{2}$$

Next, we calculate the total power of the sample and any RMS amplitude. This allows us to discard any windows with very large RMS or low power which are normally used due

to artifact noise or motion:

$$P_{\text{total}} = \sum_{n=0}^{N-1} x_{\text{center}}[n]^2 \qquad \text{RMS} = \sqrt{\frac{P_{\text{total}}}{N}} \tag{3}$$

To keep computation quick, we don't run a full fourier transform, but instead use Goertzel's algorithm to calculate power at our alpha and theta frequencies. We add these two and compare with our total power from above to create our band ratio. A small ϵ is added to avoid any division by zero:

$$P_{\theta\alpha} = P_{\theta}(6\,\text{Hz}) + P_{\alpha}(10\,\text{Hz}) \qquad \text{band\_ratio} = \frac{P_{\theta\alpha}}{P_{\text{total}} + \varepsilon} \tag{4}$$

2.6.3 Baseline and dynamic threshold

This band ratio is our main factor in asserting drowsiness. If the ratio increases above a threshold, we trigger an alert. However, our observations showed a simple number on the threshold caused too many inconsistencies with multiple users. Therefore, at the start of each session, the firmware calculates a baseline mean for each user. The first 10 seconds (2500 samples) are used to calculate a dynamic ratio of the user in an alert and awake state. This baseline gives a user-specific value to compare with when running tests:

$$\text{baseline\_mean} = \frac{1}{N_b} \sum_{i=1}^{N_b} \text{band\_ratio}_i \tag{5}$$

In the detection phase, the threshold is computed as follows where Δ is a small tuned offset (0.2 - 0.4):

$$\text{thr} = \max\big(\text{baseline\_mean} + \Delta,\ \text{BAND\_RATIO\_THRESHOLD}\big) \tag{6}$$

This results in a dynamic threshold relative to each user and their baseline 'awake' state. This has allowed us to accurately detect drowsiness in multiple users across a series of tests.

2.6.4 Drowsiness decision making

Finally, once all the digital signal processing is complete, each window is classified as *drowsy* or *not drowsy* by comparing its band ratio with the threshold. The firmware maintains a *drowsiness_counter* that increments and decrements with every window. To implement hysteresis and increase alert accuracy, a single *drowsy* window will not trigger an alert. The firmware must flag at least 3 consecutive windows as drowsy to trigger an alert. When this condition is met, the buzzer produces an audible alert and cooldown logic prevents repeated firing every window.

2.6.5 Logging and runtime

To support verification and analysis, our firmware prints strucutred debug lines over the SWV ITM Data console:

```
samples=484, fs=250.75 Hz, DRDY_overrun=0, T_min=3 ms, T_max=4 ms, win_proc=6 ms, alerts=0

W,ratio=1.2244,rms=2.019e-06,total=1.043e-09,counter=0,alert=0,thr=1.8000,base=1.224 (warming)

Baseline mean ratio=2.194 (count=10)

E, t=19979 ms, ratio=3.3240, thr=2.3940, rms=4.048e-05, counter=2, alerts=1, base=2.194
```

Figure 2: Picture showing debug prints in real time from the STM32 microchip

3 Verification

The verification stage focused on evaluating whether the final system met the primary performance requirements defined in the design review. All tests were conducted using available course-level equipment and within the practical constraints of time, budget, and component availability. While the design performed well overall, some measurements naturally reflected real-world effects such as parasitics, component tolerances, and aging, leading to small deviations from ideal specifications. Nonetheless, the results were sufficient to confirm that the system met its intended functionality, with detailed data and supporting analysis provided in the following sections and appendix A.

3.1 Power subsystem

The requirements for the power subsystem was chosen with regard to the importance of the functionality of the device. The requirement verification table shows our main goals for this subsystem and how we intend to verify them.

Requirements	Verifications	Success Criteria
Provide a minimum of 8 hours of continuous operation	• Power the system with just fully charged battery • Record how long before battery voltage drops below 3.2V	• The recorded time is more than 8hrs.
Maintain regulated voltage of 3.3V and 5V	• Observe 3.3V and 5V signals on the oscilloscope. • Record maximum and minimum of signal	• Signal minimum and maximum do not exceed 5% of signal.
Charge the battery to 4.2V	• Charge battery using USB-A • Record voltage across battery terminals after LED lights up	• The voltage recorded is between 4.1 to 4.2V

Figure 3: Requirement and verification table for power subsystem

For the battery life requirement, the earlier suggested verification method was not able to be conducted due to time constraints. Thus, an estimate was calculated with 2 primary assumptions: the battery voltage declines linearly when supplying power to the system in the operational voltage range of 4.2 to $3.3V$; the battery heating does not affect the

discharge behavior over a small time frame. Both assumptions, although reasonable, does come with an accuracy drop. To estimate the battery life, the device was operated for 10 minutes, and a voltage drop of $0.02V$ was recorded. In terms of power, this will be equivalent to

$$P_{supplied} = 3000mAh * \frac{0.02V}{4.2V - 3.3V} = 66.67mAh \; ; \quad I_{drawn} = \frac{66.67mAh}{10min} = 400.02mA \; ; \tag{7}$$

$$t_{battery\ life} = \frac{3000mAh}{400.02mA} = 7.4996hrs \tag{8}$$

The requirement of 8 hours is not achieved, but the drop in battery life is reasonable as the initial battery rating of $3600mAh$ was not used, instead a $3000mAh$ battery was used in the final design for cost and sizing reasons.

The battery managed to produce both voltage rails when operating in nominal voltage. When referring to Figure 17, it can be seen that the battery at $3.8878V$ supplied power to both buck and boost converter to produce $3.048V$ and $5.077V$ rails for the ADS1299 and STM32F412RGT6. While the $5V$ requirement is achieved with only 1.6% error, the $3.3V$ is just outside the range with 7.64% error, but still functional. As for the final requirement, the battery management system maintains a voltage less than $4.2V$ across the battery when charging, protecting the battery from over-voltage. The requirement of LED lighting up was not able to be captured as the battery was never reached $4.2V$ after a long time of charging, Due to safety and time constraints, the battery charging was stopped. However Figure 16 shows that when a supply voltage of $8V$ was supplied, the battery charged up to $4.185V$.

3.2 Analog subsystem

The requirements for the analog subsystem (ADS1299) are as follows:

Requirements	Verifications	Success Criteria
Accurately capture EEG signals in the 0.5–13 Hz range	• Provide sinusoidal signals of frequencies from 0 to 60Hz. • Record the peak voltage	• Signal attenuation past 20Hz is more than 30dB (1:1000 ratio) • Signal attenuation past 50Hz is more than 100dB (1:100000 ratio)
Amplification of the input signal by 10^3 with minimal distortion	• Provide sinusoidal signals in microvolt range • Record the peak output voltage	• The output-to-input ratio is around 1000.
Digital conversion occurs at over 240 Hz to prevent aliasing and maintain signal integrity.	• Probe the active low DRDY pin of ADS1299 during operation • Measure the period of the obtained signal	• The sampling rate is the inverse of the period obtained.

Figure 4: Requirement and verification table for analog subsystem

Unfortunately, our UART pins on the STM32 were not enabled, therefore we could not produce full fourier transform or bode plots showing our frequency range from the ADS 1299. However, we were able to accurately calculate power from 6Hz and 10hz frequency bins.

The plot in Figure 23 shows the sampling rate of all our user tests. As you can see the frequency stays near constant at 250Hz, which is above our requirement. The small dips are due to our debugger. Since we logged all data from user trials, the ST-Link connection to the SWV Data console causes delays and jitters. This resulted in our prints for sampling rate dropping, however our ADS1299 chip was configured to 250 samples per second at boot up.

3.3 Controller subsystem

The requirements for the controller subsystem (STM32F412RGT6) are as follows:

Requirements	Verifications	Success Criteria
MCU operates at 3.3V +- 5%	• Use lab power supply and scopy • Measure using oscilloscope probes	• Observe no abrupt resets or trips • No flags by debug registers
Take every DRDY signal from ADS1299 at at least 256 samples per second (0 sample drops)	• Run for 5 minutes with data stream from ADS1299 • Measure overruns on software	• Overrun count = 0 after 5 minutes
Processing latency including DSP and decision making should be less than 2 seconds	• GPIO connection can be toggled on and off between process windows	• Low to high pulse on GPIO should be less than 2 seconds

Figure 5: Requirement and verification table for analog subsystem

The voltage requirement was measured during the power system verification and satisfied 3.3V tests.

Data overruns were near 0, except for during debugger tests and user trials, where data ready overrun was viewed at 1. Similar to the sampling frequency drops, this can be attributed to the debugger delays and jitters.

Finally, the decision making response time was much faster than we expected. Seen here in Figure 25, the processing of each sample is near 0 (3-8ms). Figure 26 and Figure 27 show the accuracy of our drowsiness detection and threshold calculation. These are samples from two users and it clearly shows alerts being triggered by our device above the threshold value. This proves the reliability and accuracy of our signals to detect drowsiness and act in a timely manner.

3.4 Action subsystem

The requirements for the action subsystem are as follows:

For the testing and demos, the buzzr

Requirements	Verifications	Success Criteria
Survive at least 1000 alert cycles with no degradation of volume or tone	• Automated cycling through STM software • Simple test script and power supply	• No drops in volume, audibility and tone frequency
System current draw is less than 15mA	• Measure current during a tune pattern (eg 10 150ms beeps) • Use power supply and Ammeter	• Meets the current limits stated

Figure 6: Requirement and verification table for action subsystem

4 Costs and Schedule

4.1 Costs

The table below highlights our total cost calculations for the project. We ordered extra parts for each component incase of issues with our PCB assembly. Therefore, multiple parts were left unused and returned by the end of our project.

Team	Salary by major	Hourly	Hours per Week	Weeks worked	Total Cost	
Nikhil Talwalkar	CE ($92,430)	44	8	6	2,112	
Senturran Elangovan	EE ($76,079)	37	8	6	1,776	
	$84,254	41	8	6	1,944	Average
					3,888	Total Costs
Part Costs						
Description	Manufacturer	Part Number	Quantity	Unit Cost	Total Cost	
Micrcontroller	STMicroelectronics NV	STM32F412RGT6	1	7.76	7.76	
ADC and signal filter chip	Texas Instruments	ADS1299	1	39.31	39.31	
Battery Charger	Analog Devices INC	LT3652	1	9	9	
Electrodes	Florida Research Instruments	TDE-202	15	0.53	7.95	
Electrode Connectors	Florida Research Instruments	TDE-205XX	3	5.45	16.35	
Buzzer	Hyuduo	B082R4S4N8 (ASIN)	10	0.856	8.56	
Nucleo Dev Board	STMicroelectronics NV	STM32F411RE	1	29.38	29.38	
Battery	MakerFocus	B0DK5BBKM5 (ASIN)	2	7.99	15.98	
USB Solder Jacks	E-outstanding	B08XJN956J (ASIN)	10	0.699	6.99	
100uF Capacitor	Samsung	1276-CL21A107MQYNNWECT-ND	6	0.96	5.76	
1nF Capacitor	Kemet	399-17883-1-ND	2	0.24	0.48	
22uF Capacitor	Samsung	1276-1100-1-ND	10	0.067	0.67	
1000pF Capacitor	Samsung	1276-1015-1-ND	10	0.007	0.07	
4.7uF Capacitor	Kemet	399-C0805C475K4RACTUCT-ND	2	0.23	0.46	
2.2uF Capacitor	Murata	490-1696-1-ND	4	0.18	0.72	
1A Fuse	Vishay	MFU08051.00CT-ND	2	0.5	1	
10pos Connector	Sullins Connector Solutions	S7043-ND	1	0.58	0.58	
Battery Connector	JST Sales America Inc	455-1564-1-ND	2	0.34	0.68	
5pos Connector	Sullins Connector Solutions	S6103-ND	1	0.38	0.38	
1.5Kohm Resistor	Yageo	311-1.5KARCT-ND	10	0.09	0.9	
3.3Kohm Resistor	Yageo	311-3.30KCRCT-ND	20	0.011	0.22	
100ohm Resistor	Yageo	311-100ARCT-ND	20	0.011	0.22	
2ohm Resistor	Vishay Dale Thin Film	764-1231-1-ND	2	1.02	2.04	
20Kohm Resistor	Yageo	311-20.0KCRCT-ND	10	0.013	0.13	
330ohm Resistor	Yageo	13-RC0805JR-13330RLCT-ND	10	0.008	0.08	
402Kohm Resistor	Yageo	311-402KCRCT-ND	10	0.011	0.11	
20Kohm Potentiometer	Bourns Inc	3266W-203LF-ND	1	3.5	3.5	
Switch	Wurth Elektronik	3266W-203LF-ND	2	0.85	1.7	
Boost IC	Texas Instruments	296-39436-1-ND	1	3.26	3.26	
Buck IC	Texas Instruments	296-19643-1-ND	1	2.44	2.44	
1A Diode	Comchip Technology	641-1312-1-ND	10	0.099	0.99	
Green LED	Lite-On Inc	160-1426-1-ND	10	0.077	0.77	
Shunt convertor (TL431)	EVVO	5272-TL431-ND	2	0.1	0.2	
10pos Debug Connector	On Shore Technology Inc	ED1543-ND	1	0.26	0.26	
USB Connector	Molex	WM8672-ND	2	1.37	2.74	
Regulator IC (LM317T)	Texas Instruments	LM317TNS/NOPB-ND	2	2.24	4.48	
JST Connector	JST Sales America Inc	455-1592-ND	10	0.66	6.6	
2.2uh Inductor	TDK Corporation	445-175069-1-ND	2	0.48	0.96	
1uh Inductor	Vishay Dale	541-1043-1-ND	2	0.89	2.89	
					34.95	Shipping
					2.97	Tariff
					8.34	Tax
					232.83	Total Part Costs
					4120.83	Final Total

Figure 7: Project cost table highlighting estimated labor costs and every part

4.2 Schedule

The table below highlights our schedule of tasks for our project.

Week of	Tasks
13-Oct	Design Document
	Order hat and finalize machine shop parts
	Finalize PCB for second pass
	Order additional parts for PCB if needed
20-Oct	Breadboard testing with electrodes
	Test BMS, buck and boost converters
	DSP on STM chip
27-Oct	Software work for STM chip
	Testing Electrode signals
3-Nov	Receive PCB
	Assemble PCB parts
	Assemble hat
10-Nov	Testing of each subsystem
	Finalize STM chip connections and firmware
	Test functionality
17-Nov	Testing phase
	Test comfort, durability, battery usage, extreme conditions
	Finalize for demo

Figure 8: Project schedule

5 Ethics and Safety

5.1 Ethical Guidelines

Our device is meant solely as an assistive aid to prevent loss of focus and microsleep. It is not a replacement for preparation and safe practices that help prevent loss of focus during hazardous situations, such as night-time driving conditions. This is in line with IEEE Code of Ethics 7.8.I.1 and ACM 1.1[3][4]. Our product will clearly list limitations in accuracy and any false negative/positive rates in line with IEEE Code of Ethics section 8.8.I.5 and ACM 1.3[3][4]. Regarding privacy and confidentiality, any EEG data used from volunteers during the development of the product is purely for research purposes and enhancement of our decision algorithms. In line with ACM 1.6 and 1.7, any EEG data received will be kept confidential, provided the person's consent is obtained[4]. Regarding fairness and non-discrimination, we will validate our product's performance across all skin tones, head sizes, hair types, etc., in line with ACM 1.4. We will document any disparities in performance and adjust our product accordingly before the final demo[4].

5.2 Safety Measures

Our device was built with user safety as the foremost priority. As this is a wearable that involves direct skin contact and battery-powered electronics, the following safety measures have been taken into consideration:

5.2.1 Battery safety

The lithium polymer battery with a Battery Management System (BMS) that provides safe battery usage, such as short-circuit, charge, and discharge protection. The device will never charge while being used to eliminate any direct mains risk.

5.2.2 Electrode safety

Our device uses passive surface electrodes, which are inherently safe and do not apply current to the skin. To ensure user comfort, we will be testing for any potential skin irritation or sensitization during extended wear. Clear instructions will be provided on cleaning practices, recommended maximum wear time, and the use of skin-safe creams or preparation practices in the rare case such symptoms are found during testing.

5.2.3 Performance Safety

In alignment with our product's intended purpose as an assistive aid and not a medical device, we clearly state that it is intended to help users maintain focus but should not be relied upon as the sole measure for preventing drowsiness. All limitations in accuracy, including false positive (alert without drowsiness) and false negative (drowsiness not

detected) rates, will be communicated transparently to users. We reiterate that the device cannot replace proper rest or safe practices.

5.2.4 Lab Safety

During design, development, and testing of our product, we will adhere to the strict UIUC and ECE445 lab safety policies. All soldering for the PCB was performed in the lab, with proper eye protection and fume absorbers. All EEG data collection with volunteers was conducted with informed consent and the right to withdraw from the test at any time.

6 Conclusion

This project was designed to build a solution to provide alerts during slips in focus and concentration. We built a wearable EEG-based drowsiness detection device that could monitor brain activity in real time, and provide timely alerts when a user begins to drift into sleep. Over the semester we have designed, fabricated a PCB, integrated analog front end (ADS1299) with an STM32 microcontroller, and completed a full DSP pipeline from raw EEG samples, to buzzer alerts. While the system is still a prototype and improvements can be made, our results show a small, battery-powered EEG device can reliably interpret brain activity for a practical use.

6.1 Accomplishments

- Successful operation of ADS1299 and STM32F412 chips using battery and regulating voltages to 3.3V and 5V.
- Accurate data acquisition of EEG signals at 250Hz with near zero data overruns.
- Reliable DSP pipeline with Goertzel-based alpha and theta wave detectors, artifact and noise checks and baseline procedures to create user-specific thresholds.
- Fast processing of drowsiness decisions and timely alerts.
- Multiple subject trials who demonstrated quick drowsiness detection and most participants rated the device as reasonably comfortable, with a buzzer sufficiently distracting.

6.2 Uncertainties

- Unfortunately our drowsy labels are not based on concrete sleep staging classifications. Tests were done with closing of eyes and slowing breathing to mimic microsleeps and drowsiness conditions
- Although most RMS and noise rejection showed promising results, not all conditions were tested such as outside noise, sweat or electrode contamination, or strong tension.
- Our subject pool was relatively small and of similar age groups (20-25). Further testing is required to determine the system's behavior on a wider demographic.

6.3 Future Work

Future versions of our device could use multiple electrode channels. Our device only used 3 electrodes for comfort (2 for electrode differential and 1 for bias). Reading more frequency bands such as gamma and beta waves with these extra electrodes would prove easier and may improve the accuracy of our detection.

Finally, the physical structure of the device could be altered. Our box holding the electronics proved to be too big for the hat and was hard to balance for some users.

6.4 Ethical considerations

Ethical considerations were presented in Section 5

References

[1] National Highway Traffic Safety Administration, *Asleep at the wheel—drowsy driving*, https://www.nhtsa.gov/risky-driving/drowsy-driving, Accessed: 2025-09-19, 2017.

[2] National Safety Council. "Drivers are falling asleep behind the wheel." Accessed: 2025-09-19. [Online]. Available: https://www.nsc.org/road/safety-topics/fatigued-driver?srsltid=AfmBOopQM_LrkpRyZjnn_0Di2_N_NdR71Iabitdn3QBl6t0cOztUTAU6.

[3] I. of Electrical and E. E. (IEEE). "IEEE Code of Ethics." Approved by the IEEE Board of Directors, Aug. 1990. Accessed: 2025-09-19. [Online]. Available: https://www.ieee.org/content/dam/ieee-org/ieee/web/org/about/corporate/ieee-code-of-ethics.pdf.

[4] Association for Computing Machinery (ACM). "Acm code of ethics and professional conduct." Accessed: 2025-09-19. [Online]. Available: https://www.acm.org/binaries/content/assets/about/acm-code-of-ethics-and-professional-conduct.pdf.

[5] I. A. Fouad, "A robust and efficient eeg-based drowsiness detection system using different machine learning algorithms," *Ain Shams Engineering Journal*, vol. 14, no. 3, p. 101 895, 2023, ISSN: 2090-4479. DOI: https://doi.org/10.1016/j.asej.2022.101895. [Online]. Available: https://www.sciencedirect.com/science/article/pii/S2090447922002064.

[6] C. Anderson et al., "Feeling sleepy? stop driving—awareness of fall asleep crashes," *Sleep*, vol. 46, no. 11, zsad136, 2023. DOI: 10.1093/sleep/zsad136.

[7] Z. Mardi, S. N. M. Ashtiani, and M. Mikaili, "Eeg-based drowsiness detection for safe driving using chaotic features and statistical tests," *Journal of Medical Signals and Sensors*, vol. 1, no. 2, pp. 130–137, 2011.

[8] New York State Governor's Traffic Safety Committee. "Drowsy driving statistics." Accessed: 2025-09-19. [Online]. Available: https://trafficsafety.ny.gov/drowsy-driving-statistics.

[9] A. Tavakoli Kashani, M. Rakhshani Moghadam, and S. Amirifar, "Factors affecting driver injury severity in fatigue and drowsiness accidents: A data mining framework," *Journal of Injury & Violence Research*, vol. 14, no. 1, pp. 75–88, 2022. DOI: 10.5249/jivr.v14i1.1679.

Appendix A

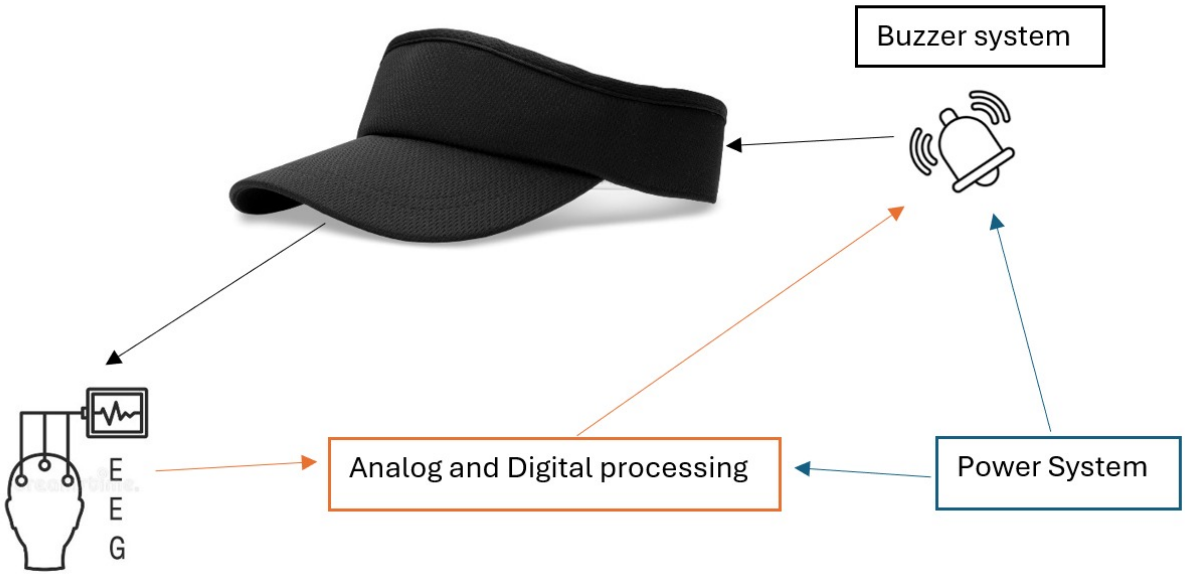

Figure 9: Visual representation of the physical device design

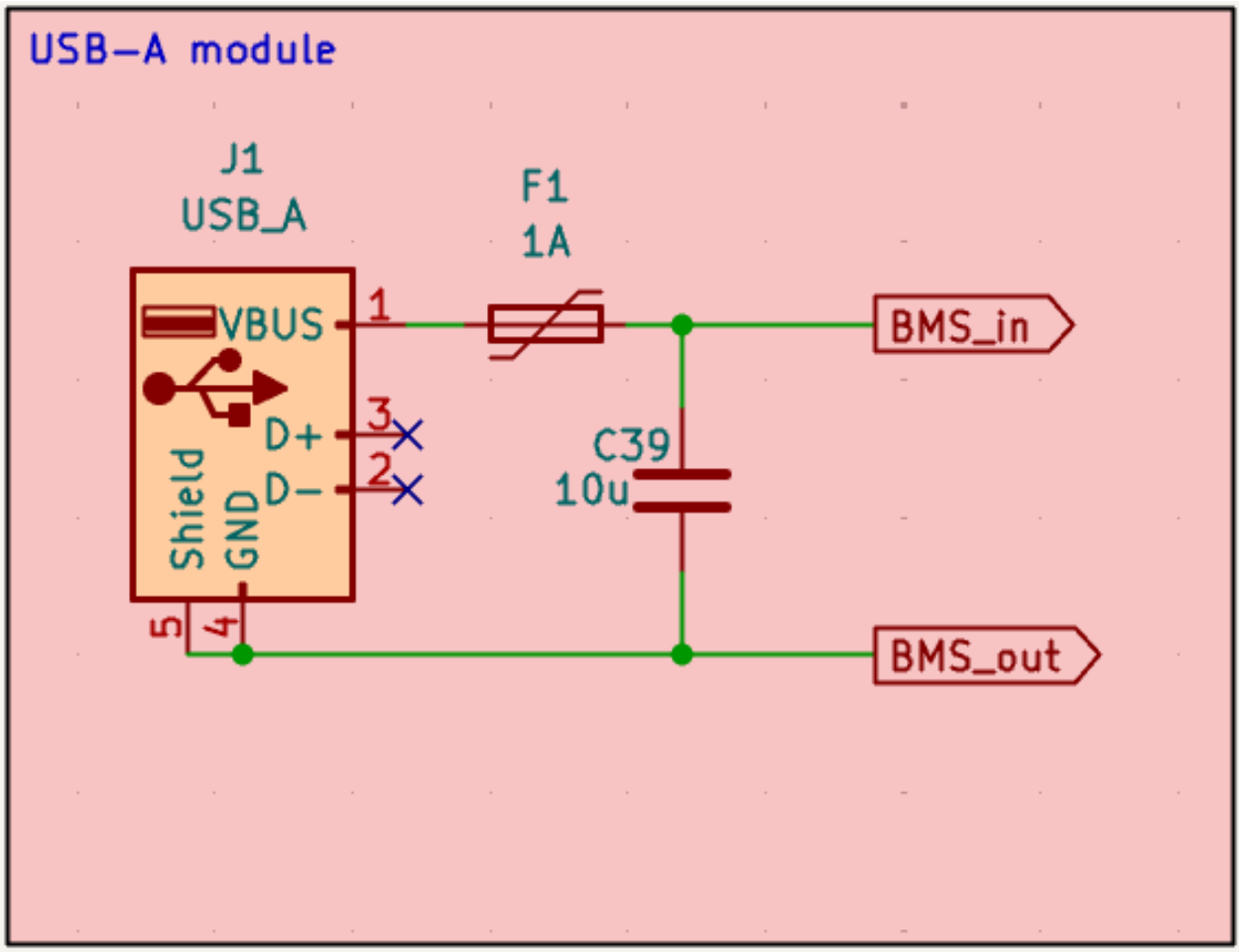

Figure 10: USB-A module schematics

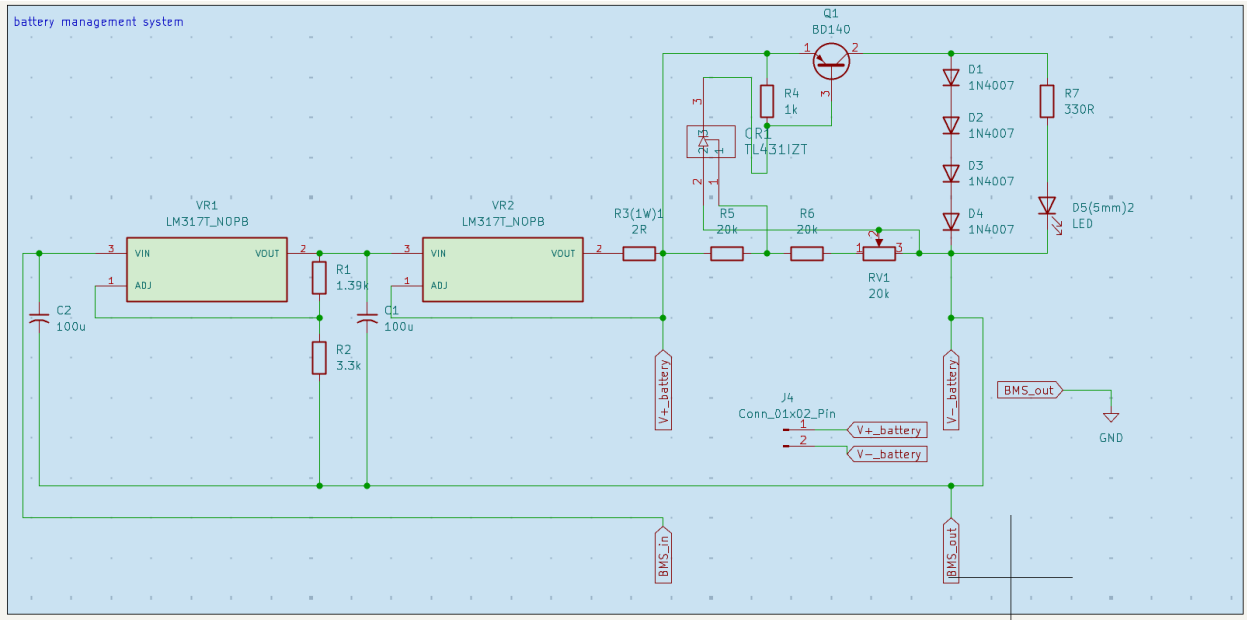

Figure 11: battery management system schematics

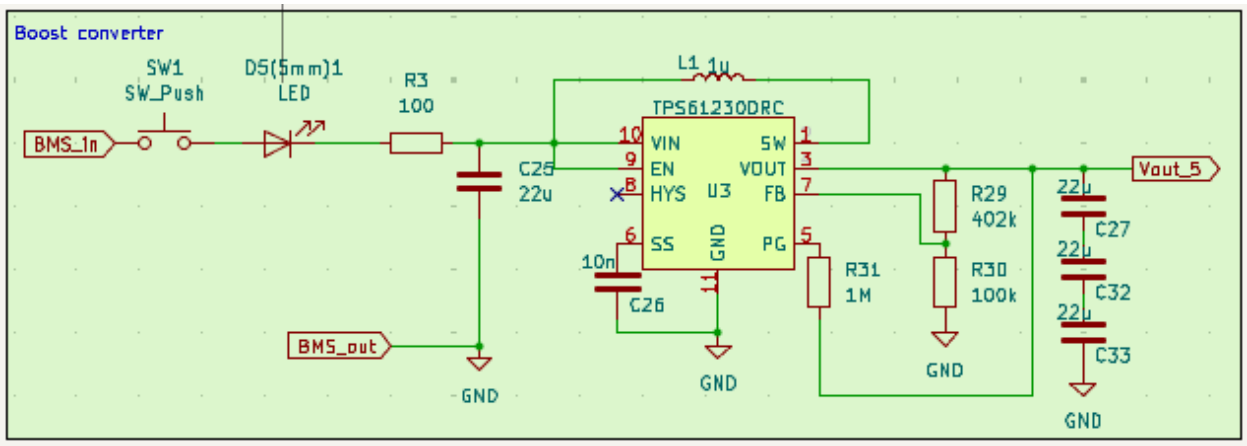

Figure 12: Boost converter schematics

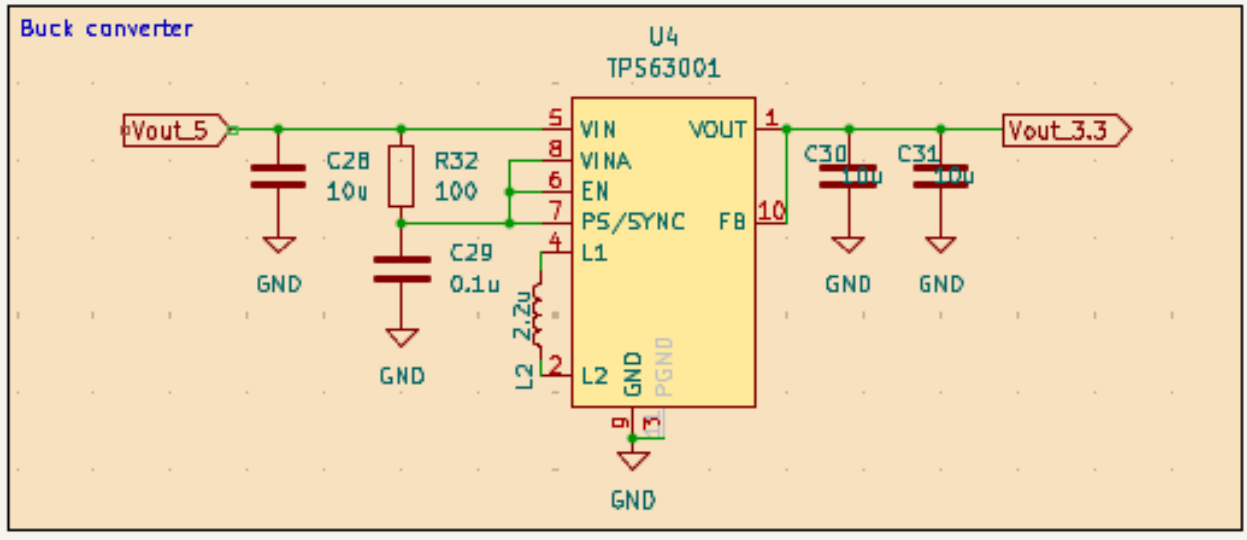

Figure 13: Buck converter schematics

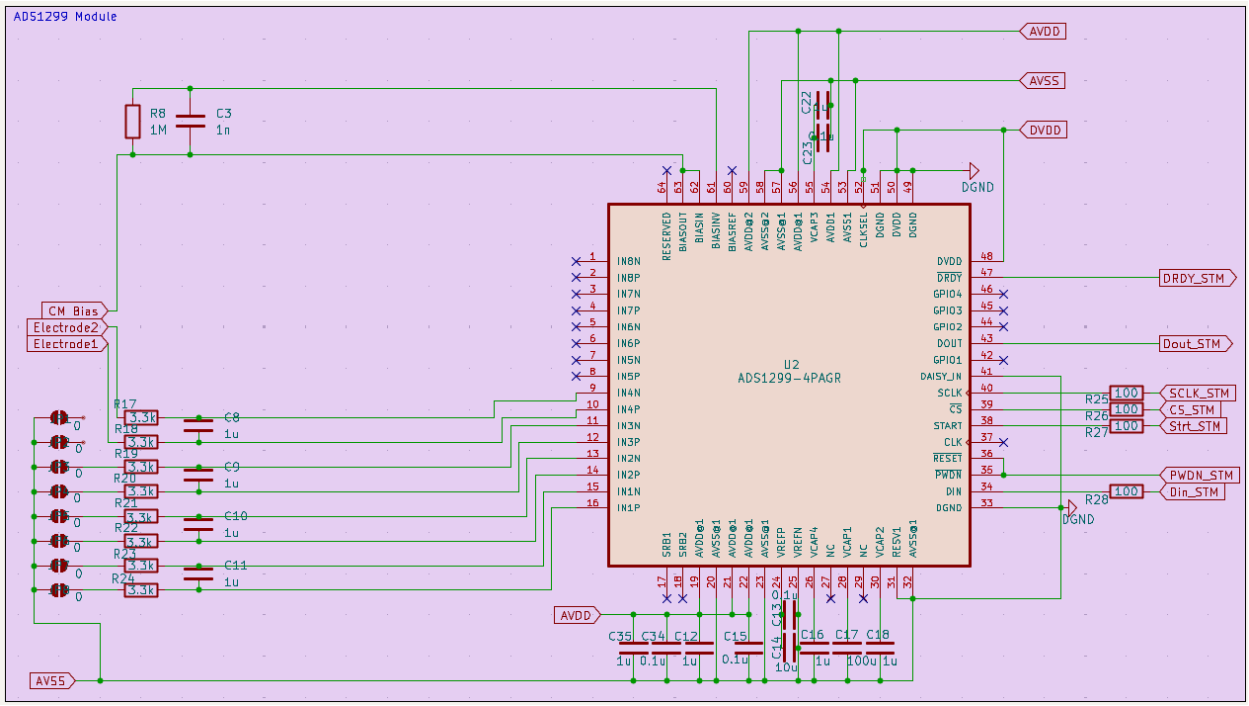

Figure 14: ADS1299 module schematics

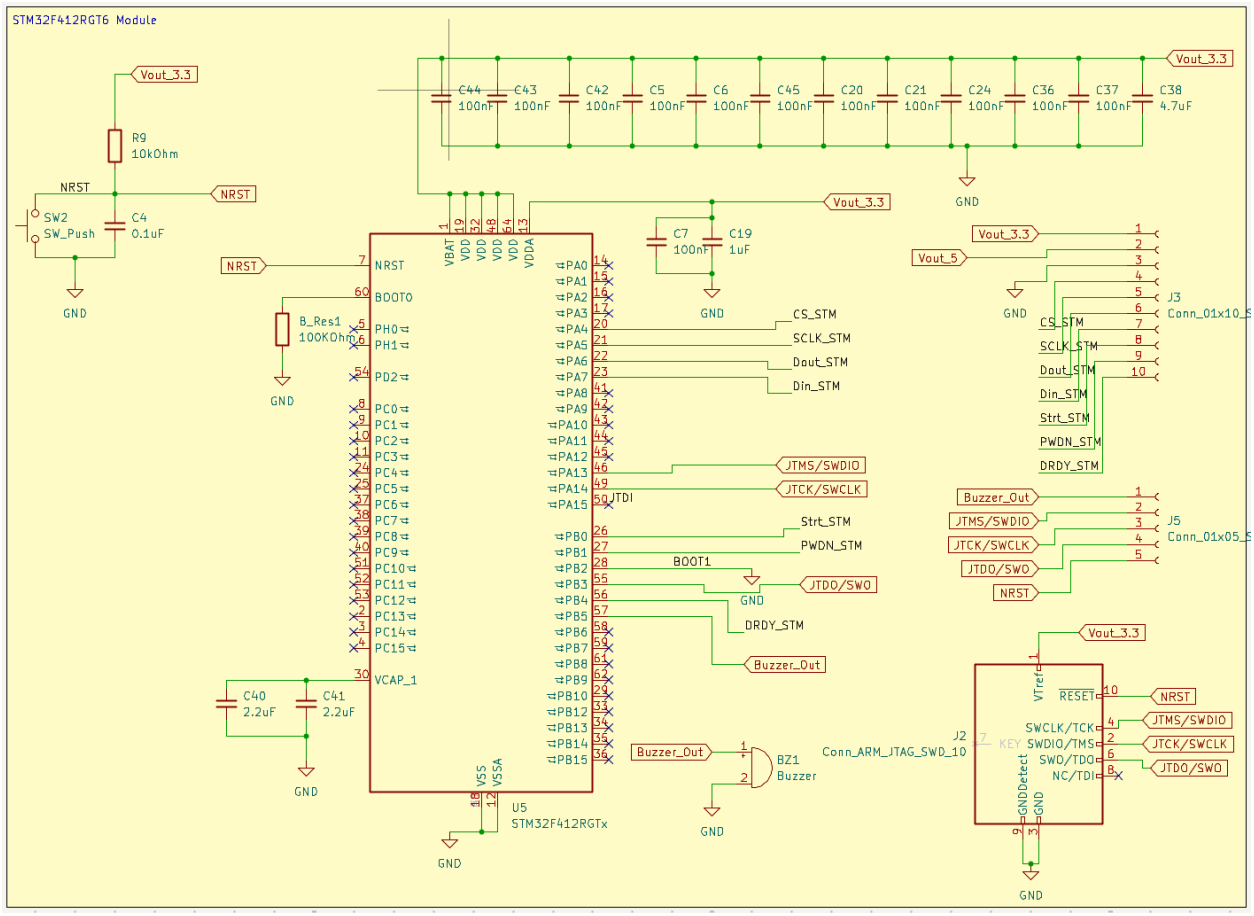

Figure 15: STM32F412RGT6 module schematics

Figure 16: Charging with $8V$ across USB-A V_{bus} and ground records a $4.14V$ potential difference across the battery terminals to allow constant voltage charging

Figure 17: $3.8878V$ battery voltage is successfully converted to $5.0776V$ and $3.048V$ voltage rails

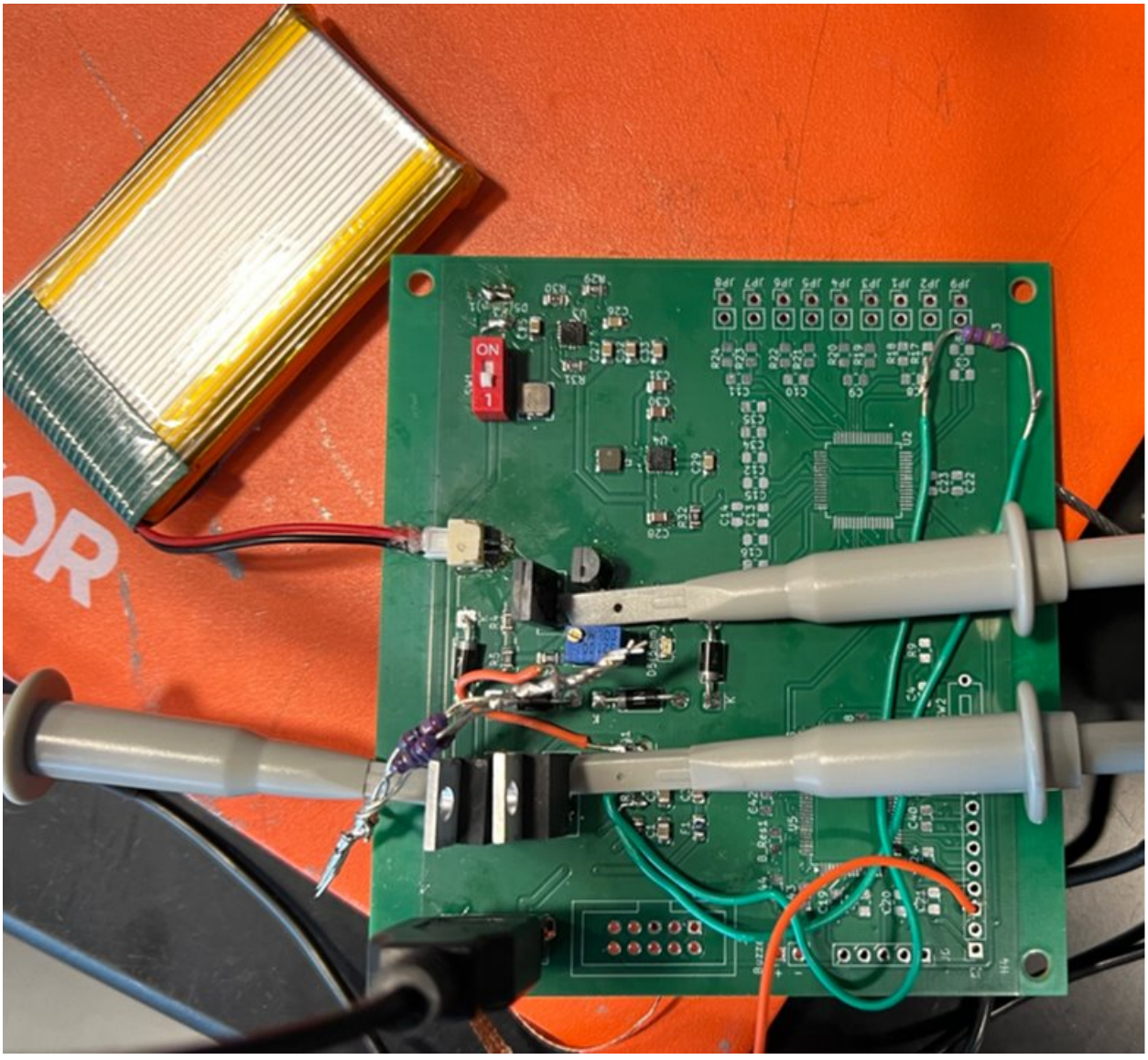

Figure 18: Probing and testing power subsystem on PCB

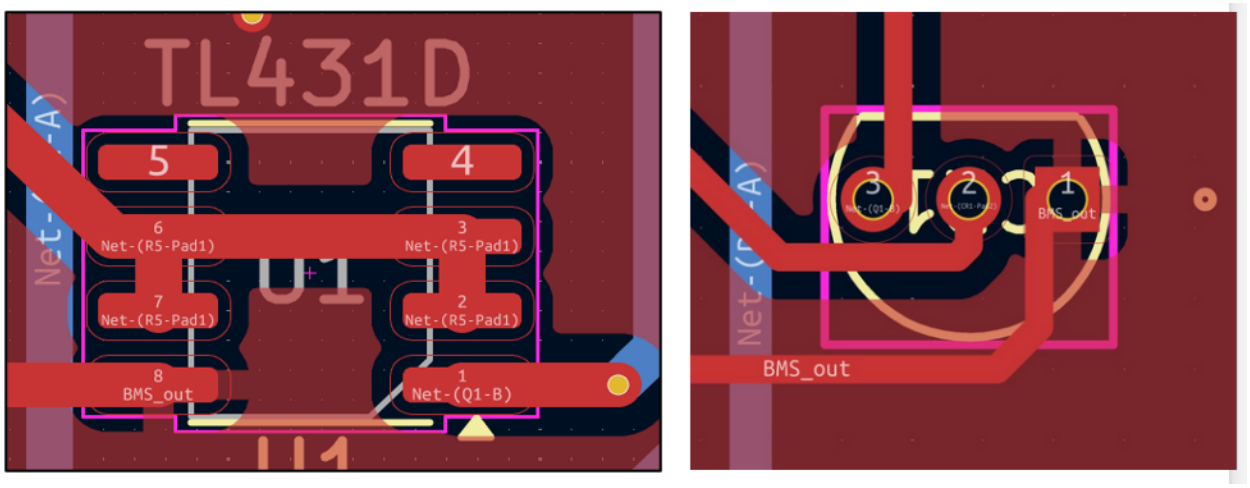

Figure 19: PCB design change for TL431D shunt voltage regulator footprint, old(left) to new(right)

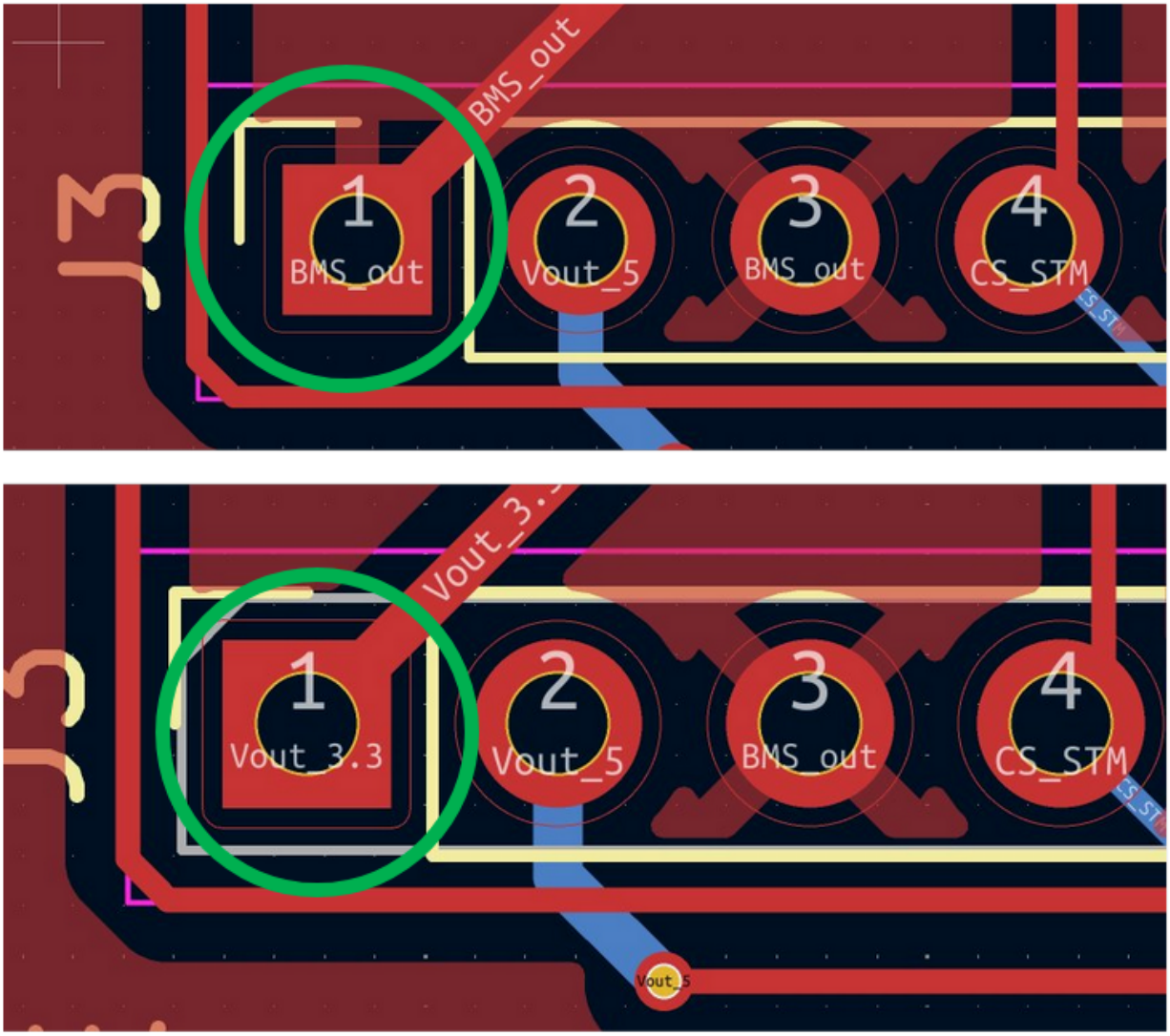

Figure 20: PCB design change to prevent connection mismatch, shorting ground to 3.3V rail, old(above) to new(below)

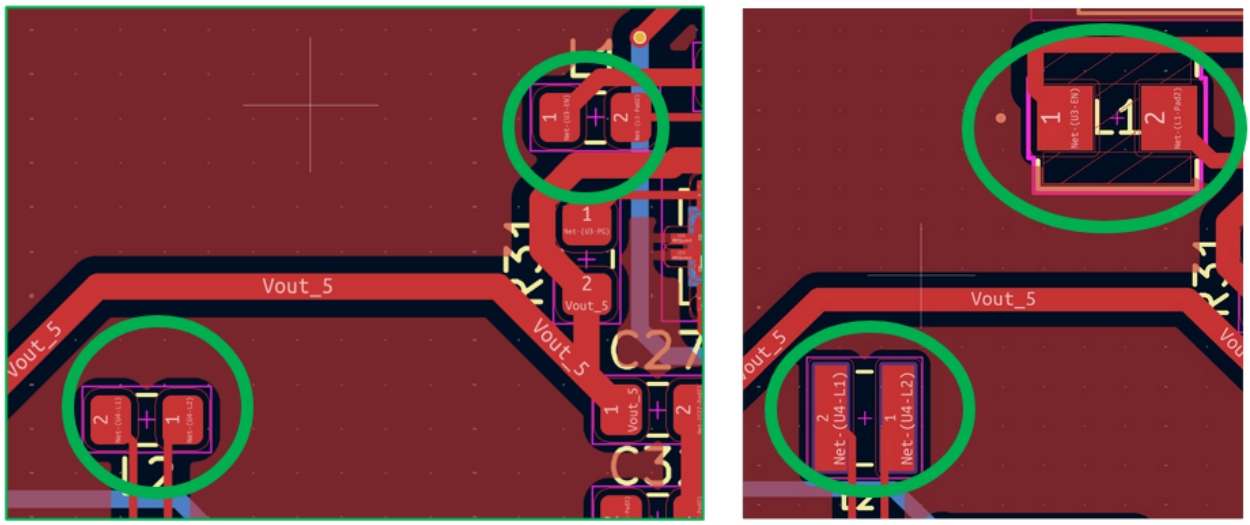

Figure 21: PCB design change to accommodate bigger inductor for power converters, old(left) to new(right)

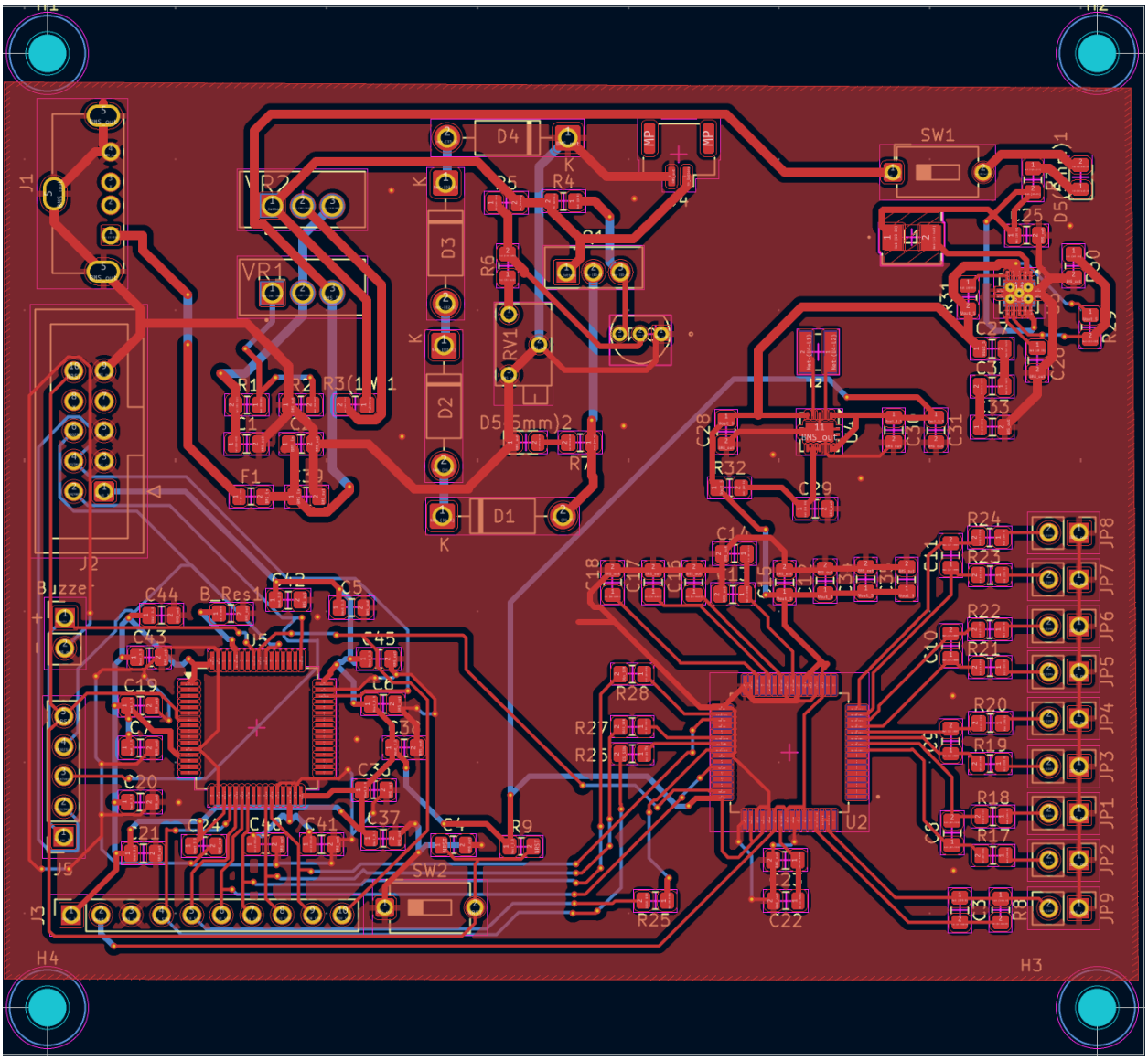

Figure 22: Final PCB design

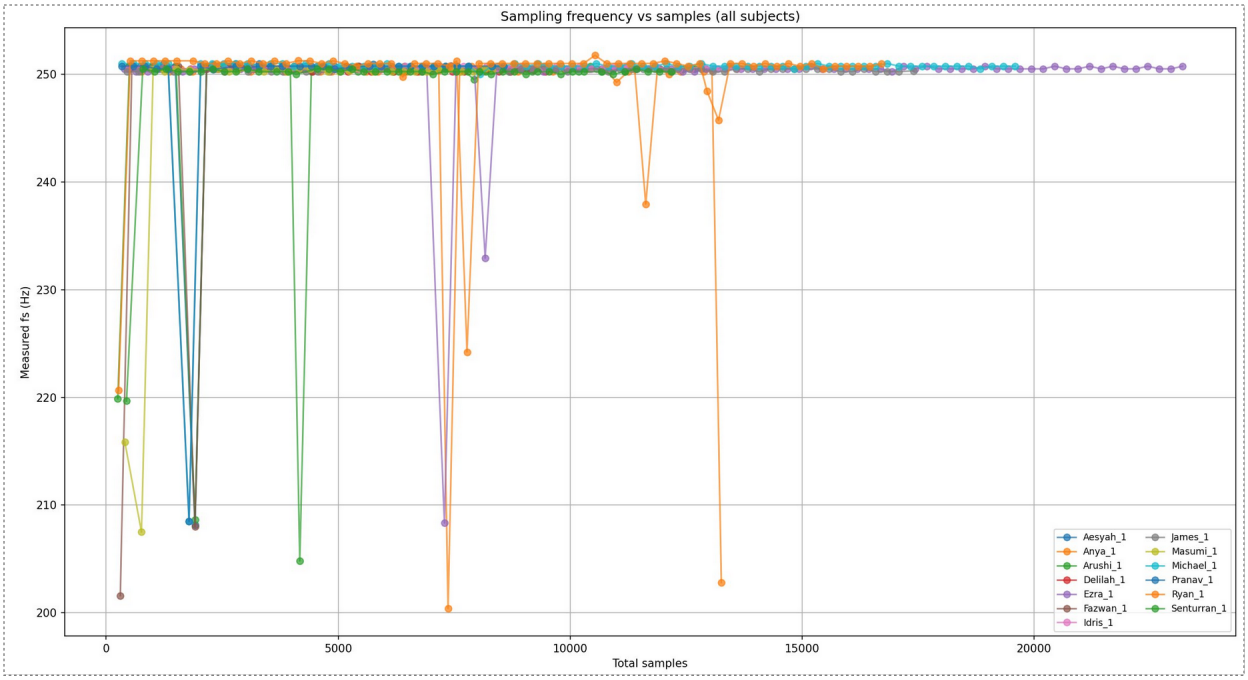

Figure 23: Sampling Frequency vs Samples

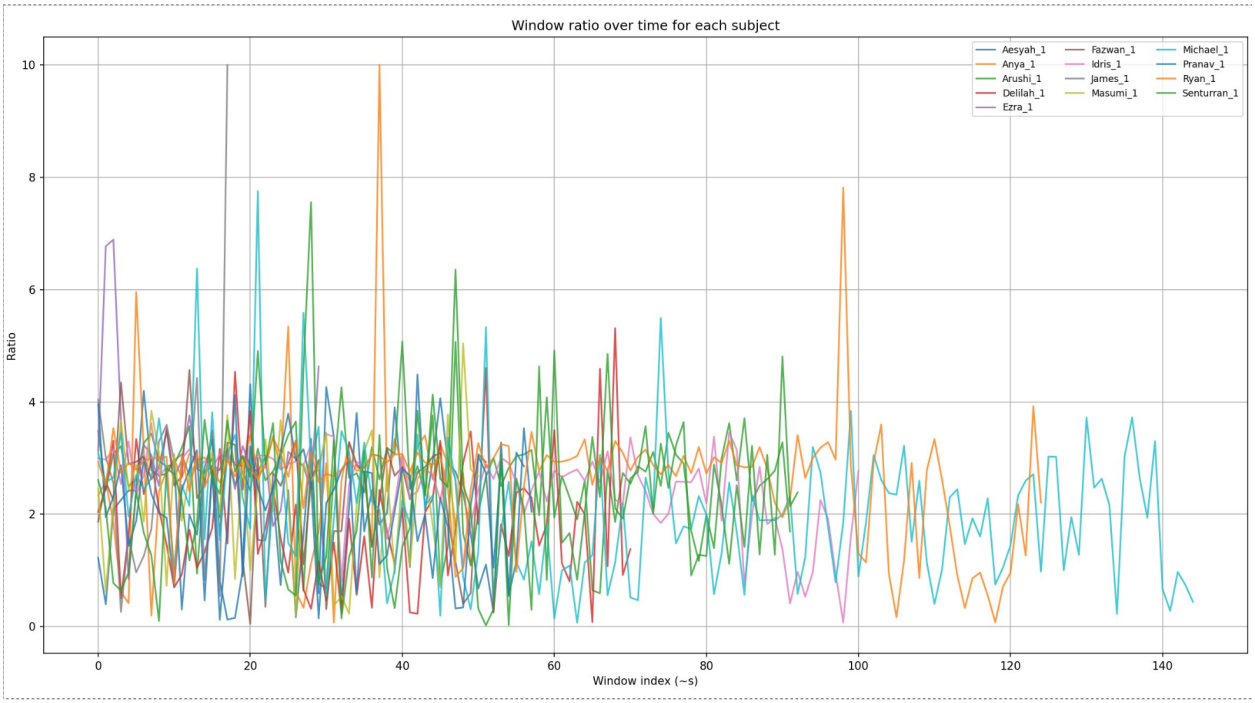

Figure 24: Window ratio over time

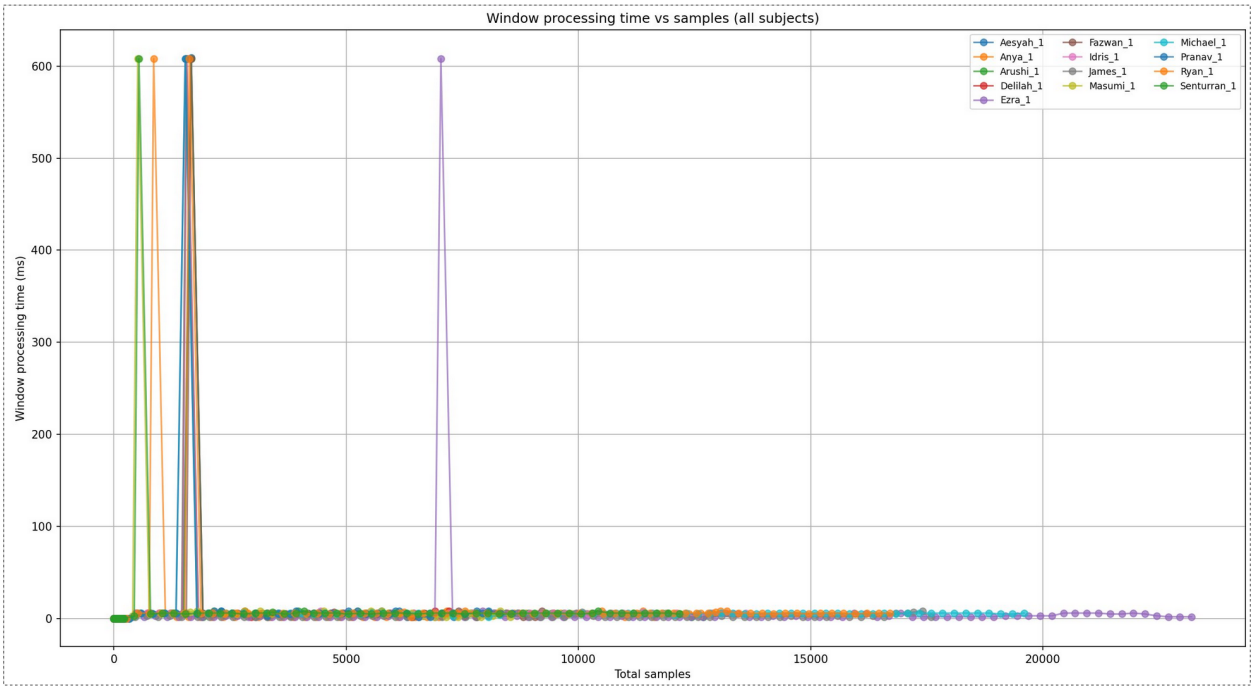

Figure 25: Window processing against samples

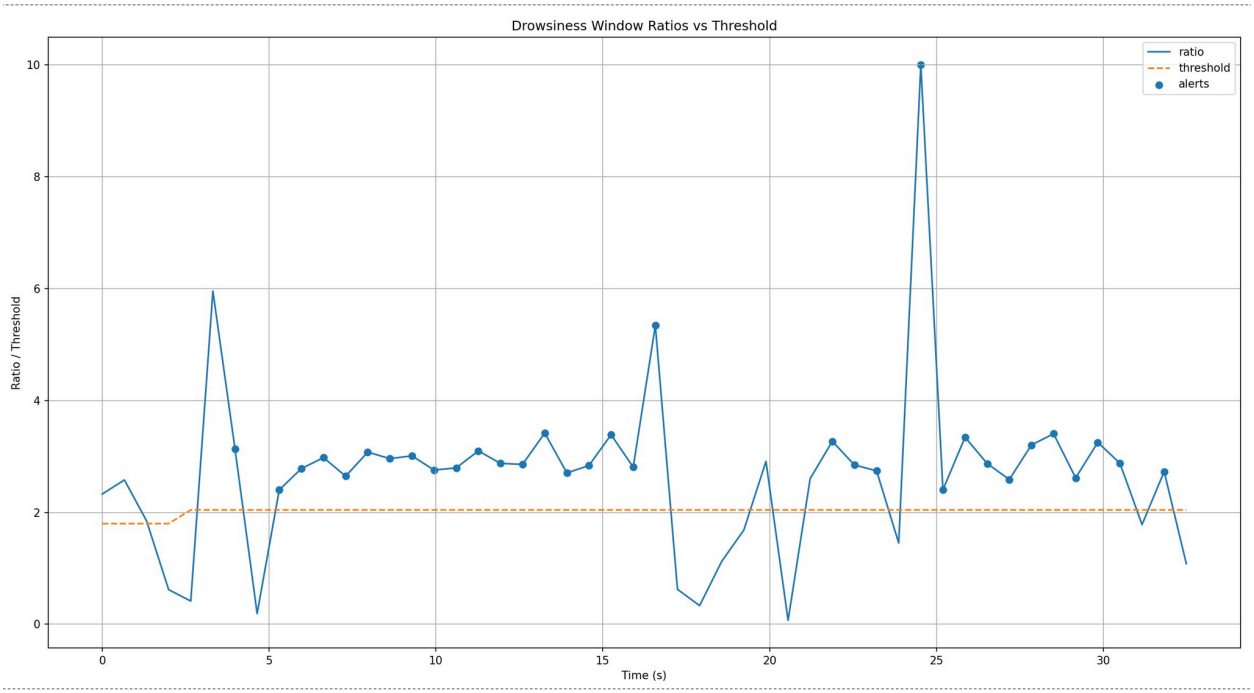

Figure 26: Drowsiness Window VS threshold for Anya

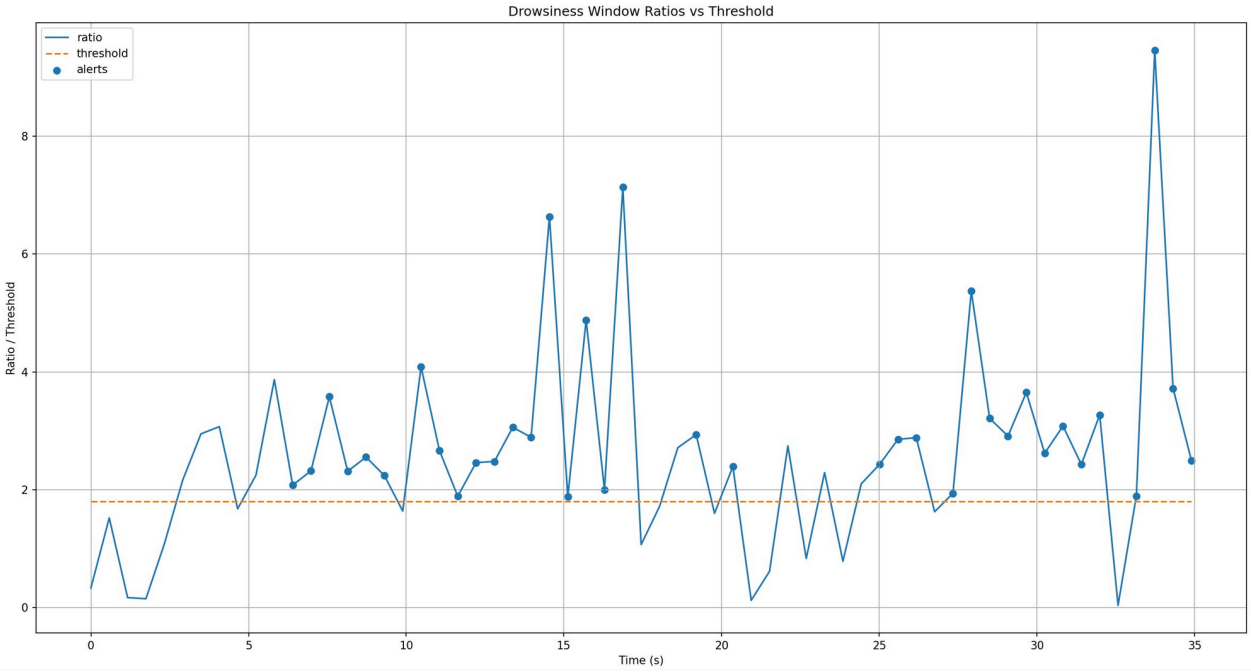

Figure 27: Drowsiness Window VS threshold for Arushi

A.1 References

[4] [5] [6] [3] [7] [1] [2] [8] [9]